



Published in final edited form as:

Cancer Prev Res (Phila). 2010 April ; 3(4): 484–494. doi:10.1158/1940-6207.CAPR-09-0250.

Sulforaphane Inhibits Constitutive and Interleukin 6 Induced Activation of Signal Transducer and Activator of Transcription 3 in Prostate Cancer Cells

Eun-Ryeong Hahm and Shivendra V. Singh

Department of Pharmacology & Chemical Biology, and University of Pittsburgh Cancer Institute, University of Pittsburgh School of Medicine, Pittsburgh, PA

Abstract

D,L-Sulforaphane (SFN), a synthetic analogue of broccoli-derived L-isomer, inhibits viability of human prostate cancer cells and prevents development of prostate cancer and distant site metastasis in a transgenic mouse model. However, the mechanism underlying anticancer effect of SFN is not fully understood. We now demonstrate that SFN inhibits constitutive and interleukin 6 (IL6)-inducible activation of signal transducer and activator of transcription 3 (STAT3), which is an oncogenic transcription factor activated in many human malignancies including prostate cancer. Growth suppressive concentrations of SFN (20 and 40 $\mu\text{mol/L}$) decreased constitutive (DU145 cells) and IL6-induced (DU145 and LNCaP cells) phosphorylation of STAT3 (Tyr705) as well as its upstream regulator Janus-activated kinase 2 (JAK2; Tyr1007/1008). Exposure of DU145 and LNCaP cells to SFN resulted in suppression of (a) IL6-induced transcriptional activity of STAT3 as judged by luciferase reporter assay, and (b) nuclear translocation of pSTAT3 as revealed by immunofluorescence microscopy. Levels of many STAT3-regulated gene products, including Bcl-2, Cyclin D1, and survivin, were also reduced in SFN-treated cells. The IL6-mediated activation of STAT3 conferred partial but marked protection against SFN-induced apoptosis as evidenced by cytoplasmic histone-associated DNA fragmentation and cleavage of poly-(ADP-ribose)-polymerase and procaspase-3. Furthermore, knockdown of STAT3 protein using siRNA resulted in a modest yet statistically significant increase in SFN-induced apoptotic DNA fragmentation in DU145 cells. Suppression of STAT3 activation was also observed in cells treated with naturally-occurring analogues of SFN. In conclusion, the present study indicates that inhibition of STAT3 partially contributes to the proapoptotic effect of SFN.

Keywords

STAT3; Prostate Cancer; Sulforaphane; Chemoprevention

Introduction

Epidemiological studies suggest that dietary intake of cruciferous vegetables may lower the risk of different malignancies including prostate cancer (1–3). Antineoplastic activity of cruciferous vegetables is attributed to isothiocyanates (ITCs), which are released by myrosinase-mediated hydrolysis of corresponding glucosinolates (4). Broccoli is a rich source of (–)-1-isothiocyanato-(4R)-(methylsulfinyl)-butane (L-SFN). The L-SFN and its synthetic derivative D,L-sulforaphane (SFN) have attracted a great deal of research enquiry because of

their anticancer effects. For example, the L-SFN and SFN are equipotent inducers of quinone reductase activity in Hepa 1c1c7 hepatoma cells (5). The L-SFN or synthetic SFN has been shown to prevent chemically-induced cancer in experimental animals, including 9-10-dimethyl-1,2-benzanthracene-induced mammary cancer in rats (6), azoxymethane-induced colonic aberrant crypt foci in rats (7), and benzo[*a*]pyrene-induced forestomach cancer in mice (8). Dietary feeding of SFN and its *N*-acetylcysteine conjugate inhibited malignant progression of lung adenomas induced by tobacco carcinogens in A/J mice (9).

In addition to prevention of chemically-induced cancer in experimental animals, SFN treatment inhibits growth of human cancer cells in culture and *in vivo* (10–12). For example, growth of PC-3 human prostate cancer xenografts in athymic mice was inhibited significantly by oral or dietary administration of SFN (13,14). Oral administration of SFN inhibited incidence and/or burden of prostatic intraepithelial neoplasia and well-differentiated prostate cancer as well as pulmonary metastasis multiplicity in a transgenic mouse model in association with augmentation of natural killer cell activity (15). Mechanistic knowledge explaining anticancer effect of SFN continues to expand, but the SFN-mediated suppression of cancer cell proliferation correlates with G2/M phase cell cycle arrest (10,11,16), apoptosis induction (10,12,17), inhibition of histone deacetylase (18), and protein binding (19). Mechanistic details of some of these cellular responses have been well described. For example, the SFN-induced G2/M phase cell cycle arrest in human prostate cancer cells is caused by checkpoint kinase 2-mediated Ser216 phosphorylation of cell division cycle 25C (16). We also found that the SFN-induced apoptosis is selective towards cancer cells and intimately linked to production of reactive oxygen species (17,20,21). The SFN has been shown to inhibit activity of mitochondrial respiratory chain enzymes leading to production of reactive oxygen species (21). The SFN-mediated suppression of androgen receptor signaling in prostate cancer cells has also been demonstrated recently (22).

Signal transducer and activator of transcription 3 (STAT3) is an oncogenic transcription factor implicated in development and progression of various malignancies including prostate cancer (23). The STAT3 is constitutively activated in a variety of cancers including breast and prostate cancers, melanoma, multiple myeloma, and leukemia (23–25). The present study demonstrates that SFN treatment inhibits constitutive and interleukin-6 (IL6)-inducible activation of STAT3 in human prostate cancer cells.

Materials and Methods

Reagents

The SFN and its naturally occurring thio- (iberverin, erucin, and berteroin), sulfinyl- (iberin and alyssin), and sulfonyl-analogues (cheirolin, erysolin, and alyssin sulfone) were purchased from LKT Laboratories. Stock solution of SFN and its analogues were prepared in dimethyl sulfoxide (DMSO) and diluted with fresh media immediately before use. An equal volume of DMSO (final concentration <0.1%) was added to controls. Cell culture reagents including medium, fetal bovine serum and antibiotic mixture were purchased from Gibco, whereas IL6 was obtained from Sigma. Antibodies against phospho-STAT3 (Tyr705), phospho-JAK2 (Tyr1007/1008), total STAT3, total JAK2, cleaved caspase-3, and cleaved poly-(ADP-ribose)-polymerase (PARP) were obtained from Cell Signaling; antibodies against Mcl-1 and cyclin D1 were from Santa Cruz Biotechnology; anti-Bcl-2 antibody was from DakoCytomation; and anti-survivin antibody was from Novus Biologicals. The phospho-STAT3 (Tyr705) antibody used for immunofluorescence microscopy was from Santa Cruz Biotechnology. The STAT3-targeted small interfering RNA (siRNA) was purchased from Santa Cruz Biotechnology. A control non-specific siRNA (UUCUCCGAACGUGUC ACG UdTdT) was from Qiagen. The sequence of the STAT3 siRNA is not revealed by the supplier. SytoxGreen and Alexa Fluor 568 goat anti-rabbit antibody were from Invitrogen.

Cell culture

Prostate cancer cell lines DU145, LNCaP, PC-3, and CWR22Rv1 were purchased from the American Type Culture Collection. Cell line authentication was performed by analysis of known genetic differences (e.g., expression of androgen receptor and p53, and analysis of androgen-responsiveness). The DU145, LNCaP and PC-3 cells were cultured as described by us previously (20,26). The CWR22Rv1 cells were cultured as recommended by the supplier.

Immunoblotting

Lysates from control and SFN-treated prostate cancer cells, and prostate tumor supernatants from control and SFN-treated Transgenic Adenocarcinoma of Mouse Prostate (TRAMP) mice were prepared as described by us previously (15,27). Lysate/supernatant proteins were resolved by sodium-dodecyl sulfate polyacrylamide gel electrophoresis and transferred onto PVDF membrane. Immunoblotting was performed as described by us previously (15,27).

Reverse transcription polymerase chain reaction (RT-PCR)

Total cellular RNA was extracted from control and SFN-treated LNCaP and DU145 cells using RNeasy kit (Invitrogen). Complementary DNA was synthesized from 1–2 µg of total RNA with reverse transcriptase and oligo(dT)₂₀. The RT-PCR reaction was carried out using High Fidelity Taq polymerase (Invitrogen), gene-specific primers, and cDNA. The primers for *JAK2* were: forward 5'-GATGAGCAAGCTTTCTCACAAGC-3' and reverse 5'-GCATGGCCCATGCCAACTGTTT-3'. The primers for *GAPDH* were: forward 5'-TGATGACATCAAGAAGGTGGTGAAG-3' and reverse 5'-TCCTTGGAGGCCATGTGGGCCAT-3'. Amplification conditions for *JAK2* were 28 cycles at 94°C for 45 sec, at 58°C for 45 sec, at 68°C for 45 sec. Amplification conditions for *GAPDH* included 25 cycles at 94°C for 30 sec, 55°C for 30 sec, 68°C for 30 sec. The PCR products were resolved by 2% agarose gel pre-stained with ethidium bromide and visualized under UV illuminator.

Luciferase assay

Luciferase assay was performed to determine the effect of SFN treatment on constitutive (DU145) and IL6-induced (DU145 and LNCaP) transcriptional activity of STAT3. Briefly, cells (5×10^4 /12-well) were plated and allowed to attach by overnight incubation at 37°C. The cells were then co-transfected with 1 µg of pSTAT3-Luc plasmid encoding STAT3 responsive element and 0.1 µg of pRL-CMV plasmid using Fugene6 (Roche Applied Science) according to the manufacturer's recommendations. The pSTAT3-Luc plasmid was kindly provided by Dr. Bharat B. Aggarwal (University of Texas M.D. Anderson Cancer Center, Houston, Texas; 28). Twenty-four hours after transfection, the cells were treated with DMSO or SFN (20 or 40 µmol/L) for 12 h prior to stimulation with 10 ng/mL IL6 for 12 h in the presence of SFN. Luciferase activity was determined using a luminometer and normalized against protein concentration.

Analysis of STAT3 dimerization

Protein extracts from control and SFN-treated DU145 cells were prepared as described by Shin et al (29). Proteins were resolved by 4% non-denaturing gel electrophoresis. Proteins were transferred onto PVDF membrane and immunoblotted with the anti-STAT3 or anti-actin antibody as described above.

Immunocytochemistry for nuclear localization of pSTAT3

The effect of SFN treatment on nuclear localization of pSTAT3 was determined by immunocytochemistry. Briefly, DU145 or LNCaP cells (1×10^5 cells) were plated on

coverslips, allowed to attach by overnight incubation, and exposed to DMSO (control) or SFN for 12 h. STAT3 activation was achieved by exposure to 10 ng/mL IL6 for 15 min at the end of incubation period. The cells were fixed with 2% paraformaldehyde for 1 h at room temperature and permeabilized with 0.05% Triton X-100 for 5 min. The cells were then incubated with phosphate-buffered saline (PBS) supplemented with 0.5% bovine serum albumin and 0.15% glycine for 1 h followed by overnight incubation with anti-pSTAT3 antibody at 4°C. The cells were then treated with 2 µg/mL Alexa Fluor 568-conjugated secondary antibody (Molecular Probes) for 1 h at room temperature. After washing with PBS, the cells were counterstained with 0.5 µmol/L SytoxGreen for 3 min at room temperature. Subsequently, the cells were mounted and observed under a Leica DC300F fluorescence microscope at ×100 objective lens magnification.

RNA interference

The DU145 cells were seeded in six-well plates and transfected at 50% confluency with 100 nmol/L control siRNA or STAT3-targeted siRNA using OligofectAMINE according to the manufacturer's instructions. Twenty-four hours after transfection, the cells were treated with DMSO (control) or specified concentrations of SFN for 24 h. The cells were then collected and processed for immunoblotting of total STAT3 and analysis of cytoplasmic histone-associated DNA fragmentation. Cytoplasmic histone-associated DNA fragmentation assay was performed using a kit from Roche Applied Sciences according to the manufacturer's instructions.

Results

SFN treatment suppressed STAT3 phosphorylation in prostate cancer cells

The STAT3 activation is caused by phosphorylation at Tyr705 (23,24). Initially, we performed immunoblotting for pSTAT3 (Tyr705) using lysates from a panel of prostate cancer cell lines (CWR22Rv1, DU145, PC-3 and LNCaP) to determine constitutive activation of this transcription factor. Constitutive pSTAT3 was detectable only in the DU145 cell line with loading of up to 80 µg of the lysate protein (Fig. 1A). A 30 min exposure of serum starved (12 h starvation) cells to 10 ng/mL IL6, a known activator of STAT3 (30,31), resulted in a robust increase in Tyr705 phosphorylation of STAT3 in DU145 and LNCaP cells (Fig. 1A, lanes 2 and 4). A modest increase in pSTAT3 level following IL6 treatment was also observed in the CWR22Rv1 cell line but not in the PC-3 cells (Fig. 1A). Total STAT3 protein was detectable in every cell line except PC-3 (Fig. 1A). We selected DU145 and LNCaP cells to determine the effect of SFN treatment on constitutive and inducible activation of STAT3. As can be seen in Fig. 1B, SFN treatment reduced levels of pSTAT3 in DU145 cells in a concentration- and time-dependent manner. For example, the level of pSTAT3 was reduced by about 80–90% by a 24h exposure of DU145 cells to 20 and 40 µmol/L SFN (Fig. 1B). The SFN-mediated suppression of Tyr705 phosphorylation of STAT3 was not explained by a decrease in its protein level. Phosphorylation of STAT3 is mediated by different kinases including JAK2 (23,30, 31). We performed immunoblotting for pJAK2 (Tyr1007/1008) to determine if SFN-mediated inhibition of STAT3 activation was due to suppression of JAK2 phosphorylation. The level of pJAK2 was also reduced in a concentration- and time-dependent manner upon exposure of DU145 cells to SFN especially at the 12 and 24 h time points (Fig. 1B). Unlike STAT3, however, suppression of JAK2 phosphorylation by SFN treatment correlated with a marked decrease in its protein level (Fig. 1B). We performed RT-PCR to test whether SFN-mediated decline in JAK2 protein level was due to its reduced transcription. The level of *JAK2* mRNA, after correction for *GAPDH* control, was decreased by ~70–90% in DU145 and LNCaP cells treated for 24 h with 40 µmol/L SFN (results not shown). These results indicated that SFN treatment reduced transcription of *JAK2*.

Next, we tested the possibility whether SFN treatment affected IL6-induced activation of STAT3. For these experiments DU145 and LNCaP cells were treated with 40 $\mu\text{mol/L}$ SFN for 24 h and stimulated with 10 ng/mL IL6 for the indicated time periods at the end of incubation period. The IL6-induced phosphorylation of JAK2 as well as STAT3 was suppressed in both DU145 (Fig. 1C) and LNCaP cells (Fig. 1D). However, the LNCaP cell line (Fig. 1D) was markedly more sensitive to SFN-mediated inhibition of IL6-inducible JAK2 and STAT3 phosphorylation as well as down-regulation of total JAK2 protein expression compared with DU145 cells (Fig. 1C). The results were comparable if the cells were co-treated with SFN and IL6 for 24 h (data not shown). Collectively, these results indicated that SFN treatment inhibited constitutive as well as IL6-induced phosphorylation of STAT3 by reducing the levels of total and phospho-JAK2.

SFN treatment inhibited STAT3-dependent luciferase activity in prostate cancer cells

We performed luciferase reporter assay to determine the effect of SFN treatment on transcriptional activity of STAT3. In DU145 cells, a 24 h treatment with 40 $\mu\text{mol/L}$ SFN resulted in a modest yet statistically significant decrease in STAT3-dependent luciferase activity (~58% inhibition compared with DMSO-treated control) (Fig. 2A). As expected, transcriptional activity of STAT3 was increased in the presence of IL6 (10 ng/mL, 12 h exposure in the presence of SFN). The IL6-mediated increase in STAT3-associated luciferase activity was completely abolished in the presence of SFN (Fig. 2A). Consistent with immunoblotting data (Fig. 1D), the IL6-stimulated STAT3-dependent luciferase activity in LNCaP cells was completely abolished by a 24 h exposure to 20 and 40 $\mu\text{mol/L}$ SFN (Fig. 2B). These results indicated that SFN treatment inhibited constitutive and IL6-induced transcriptional activity of STAT3 in DU145 and LNCaP cells.

SFN treatment diminished dimerization and nuclear localization of STAT3

Phosphorylation at Tyr705 results in homodimerization of STAT3 or heterodimerization with other STATs, which enables nuclear translocation of STAT3 for binding to specific sequences of target genes (23,28,31). We designed experiments using DU145 cells to determine whether SFN treatment affected homodimerization and nuclear translocation of STAT3. As shown in Fig. 2C, electrophoresis followed by immunoblotting revealed time-dependent reduction in level of STAT3 homodimer in DU145 cells upon treatment with 40 $\mu\text{mol/L}$ SFN.

Fig. 3A depicts immunostaining for constitutive pSTAT3 (red fluorescence) and SytoxGreen-associated nuclear staining (green fluorescence) in DU145 cells following 12 h treatment with DMSO (control) or the indicated concentrations of SFN. In DU145 cells, pSTAT3 was predominantly localized in the nucleus as evidenced by yellow-orange staining due to merging of red and green fluorescence. Nuclear level of pSTAT3 was decreased markedly in cells treated with 20 and 40 $\mu\text{mol/L}$ SFN (Fig. 3A). As expected, a 15 min exposure of DU145 cells to 10 ng/mL IL6 resulted in increased nuclear level of pSTAT as evidenced by more intense yellow-orange staining (Fig. 3B) compared with unstimulated DU145 cells (Fig. 3A). The IL6-stimulated nuclear localization of pSTAT3 was also inhibited in the presence of SFN in both DU145 (Fig. 3B) and LNCaP cells (Fig. 3C) at each concentration. Nuclear staining for pSTAT3 in unstimulated LNCaP cells was practically undetectable (results not shown), which is consistent with the immunoblotting data (Fig. 1A). These results demonstrated inhibition of constitutive and IL6-induced dimerization and/or nuclear localization of pSTAT3 in the presence of SFN in DU145 and LNCaP cells.

SFN treatment altered levels of STAT3-regulated gene products in prostate cancer cells

The STAT3 is known to regulate expression of various genes involved in cell proliferation and apoptosis including Mcl-1, Bcl-2, cyclin D1, and survivin (23,28,31). To test whether SFN-mediated suppression of STAT3 activation resulted in down-regulation of its target gene

products, we performed immunoblotting for above mentioned proteins using lysates from DU145 and LNCaP cells treated with DMSO (control) and SFN. The levels of Mcl-1, Bcl-2, Cyclin D1, and survivin proteins were altered upon treatment with SFN in both cell lines, albeit with different kinetics or cell-line specificity. The SFN-mediated down-regulation of Bcl-2 and Cyclin D1 protein levels was clearly evident in both cell lines especially at the 12–24 h time points (Fig. 4A,B). The SFN treatment decreased protein level of survivin at 6–12 h time points in DU145 cells (Fig. 4A) and at 24 h time point in the LNCaP cell line (Fig. 4B). We performed additional immunoblotting analyses to test whether expression of the above proteins was regulated by IL6/STAT3 in DU145 and LNCaP cells. As can be seen in Fig. 4C expression of Mcl-1, Bcl-2, and Cyclin D1 proteins was increased by stimulation with IL6. The effect on survivin protein level was inconsistent (results not shown). The IL6-stimulated induction of Mcl-1, Bcl-2, and Cyclin D1 protein expression was attenuated to varying extent in the presence of SFN (Fig. 4C). These results indicated that the SFN-mediated suppression of STAT3 activation was accompanied by down-regulation of some of its target gene products.

IL6-induced activation of STAT3 conferred protection against SFN-induced apoptosis

To test biological significance of SFN-mediated suppression of STAT3 activation in our model, we determined apoptosis induction by SFN in LNCaP cells treated for 24 h with 20 and 40 $\mu\text{mol/L}$ in the absence or presence of 10 ng/mL IL6 (24 h treatment). As shown in Fig. 5A, the SFN treatment resulted in a concentration-dependent and statistically significant increase in cytoplasmic histone-associated DNA fragmentation, which is a highly sensitive and reliable technique for quantitation of apoptotic cell death. The apoptotic DNA fragmentation resulting from SFN treatment was partially but significantly abrogated in IL6-stimulated cells (Fig. 5A). Consistent with these results, SFN-mediated cleavage of PARP and caspase-3 was markedly inhibited in the presence of IL6 in LNCaP cells (Fig. 5B).

Effect of STAT3 knockdown on SFN-induced apoptosis in DU145 cells

We determined the effect of STAT3 protein knockdown on SFN-induced apoptosis using DU145 cells. The level of STAT3 protein was reduced by about 70% upon transient transfection of DU145 cells with STAT3-targeted siRNA in comparison with cells transfected with a control non-specific siRNA (Fig. 5C, *inset*). Knockdown of STAT3 protein in DU145 cells resulted in a modest yet statistically significant increase in SFN-induced cytoplasmic histone-associated DNA fragmentation (Fig. 5C). Collectively, these results indicated that STAT3 activation conferred partial protection against SFN-induced apoptosis in prostate cancer cells. It is also clear that the DU145 cell line is markedly more resistant to SFN-induced apoptotic DNA fragmentation (Fig. 5C) compared with LNCaP cells (Fig. 5A). Because STAT3 protein knockdown resulted in only modest increase in SFN-induced apoptosis in DU145 cells, our interpretation is that differences in constitutively active STAT3 levels between these cell lines may only partially account for differential sensitivity of these cells to SFN-induced apoptosis. At the same time, the possibility that complete knockdown of STAT3 protein results in a greater sensitization of DU145 cells to SFN-induced apoptosis can't be fully discarded.

Effect of oral SFN administration on levels of total and phospho-STAT3/JAK2 in prostate tumors of TRAMP mice

We have shown previously that oral administration of SFN retards development of prostate cancer in TRAMP mice (15). We used the prostate tumor tissues harvested from representative control and SFN-treated TRAMP mice to determine effect on total and/or phospho-STAT3/JAK2 levels. As shown in Fig. 5D, the prostate tumors from SFN-treated TRAMP mice exhibited a decrease in levels of pSTAT3 (~20% decrease), total STAT3 (~30% decrease), and total JAK2 (~70% decrease) compared with controls. Expression of phospho-JAK2 was not

detectable in the prostate tumors of either control or SFN-treated TRAMP mice (results not shown). These results indicated that SFN administration reduced levels of total and/or phospho-STAT3/JAK2 in prostate tumors of TRAMP mice.

Structure-activity relationship for effect of SFN analogues on pSTAT3 and pJAK2

We used naturally-occurring thio-, sulfinyl-, and sulfonyl-analogues of SFN (please refer to Fig. 6A for chemical structures of the analogues) to determine possible impact of oxidation state of sulfur and alkyl chain length on thioalkyl isothiocyanate-mediated inhibition of STAT3/JAK2 phosphorylation. As can be seen in Fig. 6B, inhibition of JAK2 and STAT3 phosphorylation as well as JAK2 down-regulation was also observed in cells treated for 24 h with SFN analogues. Even though a clear structure-activity relationship was not discernible, suppression of STAT3 phosphorylation at 20 $\mu\text{mol/L}$ concentration was more pronounced for SFN compared with other compounds. In general, the sulfonyl derivatives (Cheirolin, Erysolin, and Alyssin sulfone) were relatively weak suppressors of STAT3 phosphorylation compared with SFN despite potent inhibition of JAK2 phosphorylation. These results suggest that the sulfonyl derivatives might activate other kinases (e.g., Src) to counteract inhibition of JAK2 phosphorylation.

Discussion

The STAT3, a nuclear transcription factor belonging to the seven member STAT gene family of transcription factors, plays an important role in promotion of growth and progression of prostate cancer (24,25,32–35). The STAT3 is constitutively active in clinical human prostate cancer (33,35). For example, Dhir et al (33) observed significantly higher levels of constitutively active STAT3 in both prostate carcinomas and the matched normal prostate tissues adjacent to tumors compared to the normal prostates from donors without prostate cancer. However, no correlation was noted between STAT3 activation and Gleason grade or serum prostate specific antigen levels (33). Several reports also indicate that STAT3 promotes proliferation and inhibits apoptosis in cultured prostate cancer cells (24,36). Moreover, STAT3 is implicated in transition of hormone-sensitive prostate cancer to androgen-independent state (also referred to as “castration-resistant” or “hormone-refractory”) (25,36), which is highly aggressive and resistant to chemotherapy (37). Accordingly, agents that are relatively safe but could suppress activation of STAT3 are highly attractive for both prevention of prostate cancer and treatment of castration-resistant disease. The present study demonstrates that SFN, a promising cancer chemopreventive agent, inhibits both constitutive and IL6-induced activation of STAT3 in human prostate cancer cells regardless of their androgen-responsiveness. The SFN-mediated suppression of STAT3 activation in human prostate cancer cells is evident at pharmacologically relevant concentrations based on our own pharmacokinetic data. We have shown previously that gavage with a single dose of 6 μmol SFN results in peak plasma concentration of about 19 $\mu\text{mol/L}$ in mice (15).

Activation of STAT3 entails phosphorylation on a critical tyrosine residue (Tyr705), which is mediated by different kinases including JAKs, Rac1, and Src (23,28,31,38). The IL6-mediated activation of STAT3 is regulated by JAKs through cytoplasmic domain of gp130 of the IL6 receptor (39). The present study reveals that SFN-mediated inhibition of STAT3 activation in prostate cancer cells is accompanied by suppression of constitutive as well as IL6-inducible Tyr1007/1008 phosphorylation of JAK2. The time course-kinetics of SFN-mediated suppression of pJAK2 mirrors that of pSTAT3 inhibition. The mechanism by which SFN inhibits JAK2 phosphorylation seems to involve transcriptional repression of *JAK2* leading to a reduction in its protein level. Inhibition of STAT3 activation in DU145 cells by a naturally-occurring structural analogue of SFN (phenethyl isothiocyanate) was reported recently during completion of our work (40). However, unlike our results, the phenethyl isothiocyanate-

mediated suppression of STAT3 activation was not due to a decrease in level of JAK2 protein (40). These observations underscore mechanistic differences between structurally-related SFN and phenethyl isothiocyanate. Recent studies from our laboratory have documented additional unique mechanistic differences between SFN and phenethyl isothiocyanate. For example, SFN causes autophagy that serves to protect prostate cancer cells against apoptosis (41). On the other hand, autophagy induction seems to contribute to the overall cell death caused by phenethyl isothiocyanate (42).

The Tyr705 phosphorylation of STAT3 causes its homodimerization (28,31). The STAT3 dimer translocates to the nucleus for binding to specific DNA sequences in the promoter of target genes (28,31). The present study indicates that the SFN-mediated inhibition of STAT3 phosphorylation suppresses its transcriptional activity as evidenced by: (a) inhibition of constitutive and IL6-inducible STAT3-dependent luciferase reporter activity in the presence of SFN, (b) a reduction in level of constitutive STAT3 homodimer in SFN-treated DU145 cells, (c) a decrease in constitutive and IL6-stimulated nuclear translocation of pSTAT3 upon treatment with SFN, and (d) suppression of many STAT3 regulated gene products (e.g., Cyclin D1 and survivin) in SFN-treated DU145 and LNCaP cells.

The present study also addresses the question of whether suppression of STAT3 activation contributes to apoptotic cell death resulting from SFN exposure. The IL6-stimulated activation of STAT3 confers partial yet significant protection against SFN-induced apoptosis in both LNCaP (Fig. 5A) and DU145 cells (results not shown). Knockdown of STAT3 results in only modest increase in SFN-induced apoptosis in DU145 cells, which could be attributed to incomplete knockdown of the STAT3 protein. Alternatively, the possibility that suppression of STAT3 only partially accounts for SFN-induced apoptosis in prostate cancer cells is also likely. To this end, we have shown previously that SFN treatment causes generation of reactive oxygen species leading to activation of mitochondria-mediated apoptosis in PC-3 and LNCaP human prostate cancer cells (20,21).

In conclusion, the present study provides experimental evidence to indicate that cancer chemopreventive agent SFN causes suppression of constitutive as well as IL6-induced activation of STAT3 in human prostate cancer cells irrespective of their androgen-responsiveness. Moreover, the IL6-mediated activation of STAT3 activation confers partial yet statistically significant protection against SFN-induced apoptosis.

Acknowledgments

We thank Dr. Bharat B. Aggarwal (University of Texas M.D. Anderson Cancer Center, Houston, Texas) for the generous gift of pSTAT3-Luc plasmid.

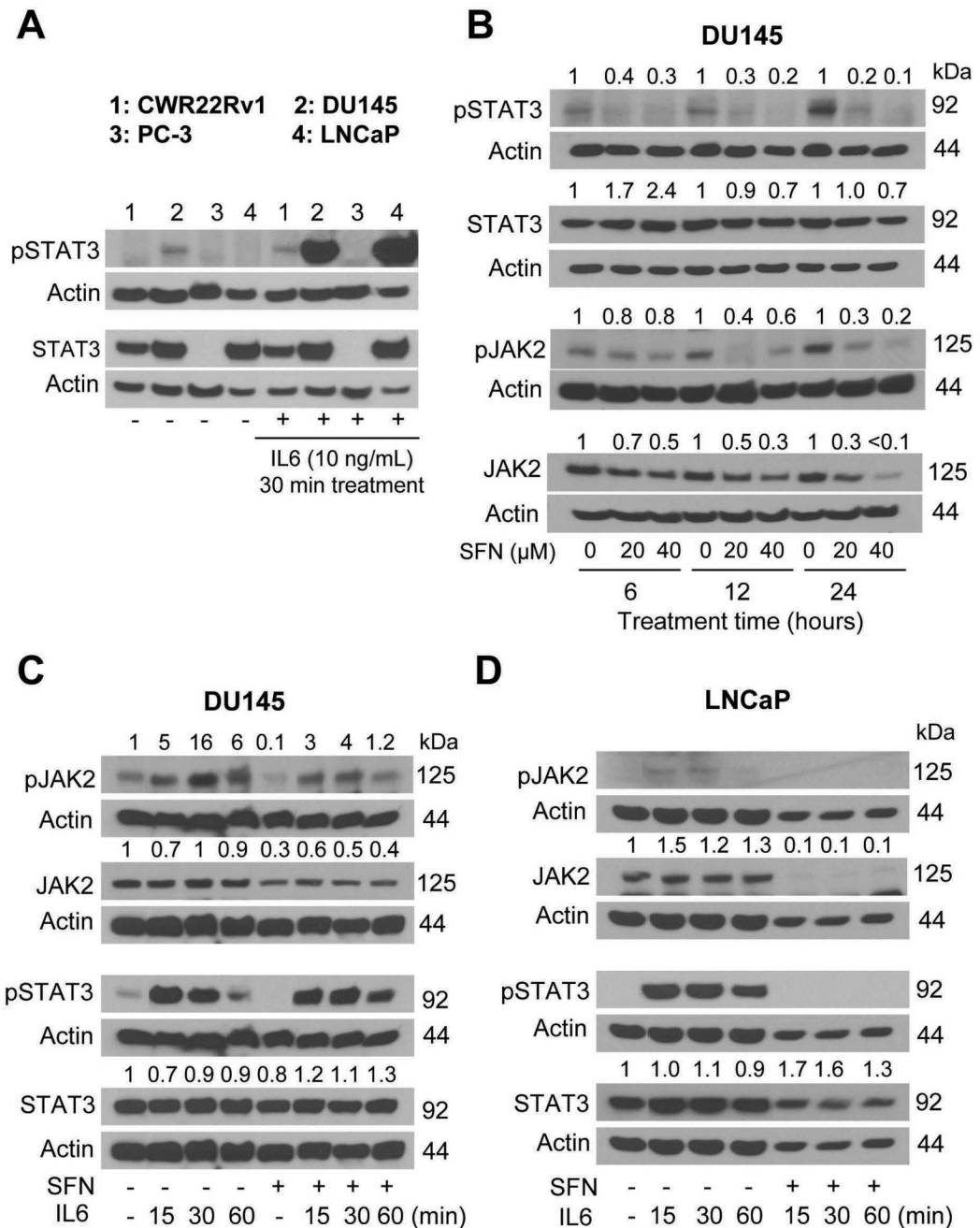
Grant Support: This study was supported by USPHS grants CA115498-05 and CA101753-07 awarded by the National Cancer Institute.

References

1. Verhoeven DT, Goldbohm RA, van Poppel G, Verhagen H, van den Brandt PA. Epidemiological studies on *Brassica* vegetables and cancer risk. *Cancer Epidemiol Biomarkers Prev* 1996;5:733–748. [PubMed: 8877066]
2. Kolonel LN, Hankin JH, Whittemore AS, et al. Vegetables, fruits, legumes and prostate cancer: a multiethnic case-control study. *Cancer Epidemiol Biomarkers Prev* 2000;9:795–804. [PubMed: 10952096]
3. Ambrosone CB, McCann SE, Freudenheim JL, Marshall JR, Zhang Y, Shields PG. Breast cancer risk in premenopausal women is inversely associated with consumption of broccoli, a source of isothiocyanates, but is not modified by GST genotype. *J Nutr* 2004;134:1134–1138. [PubMed: 15113959]

4. Hecht SS. Inhibition of carcinogenesis by isothiocyanates. *Drug Metab Rev* 2000;32:395–411. [PubMed: 11139137]
5. Zhang Y, Talalay P, Cho CG, Posner GH. A major inducer of anticarcinogenic protective enzymes from broccoli: isolation and elucidation of structure. *Proc Natl Acad Sci USA* 1992;89:2399–2403. [PubMed: 1549603]
6. Zhang Y, Kensler TW, Cho CG, Posner GH, Talalay P. Anticarcinogenic activities of sulforaphane and structurally related synthetic norbornyl isothiocyanates. *Proc Natl Acad Sci USA* 1994;91:3147–3150. [PubMed: 8159717]
7. Chung FL, Conaway CC, Rao CV, Reddy BS. Chemoprevention of colonic aberrant crypt foci in Fischer rats by sulforaphane and phenethyl isothiocyanate. *Carcinogenesis* 2000;21:2287–2291. [PubMed: 11133820]
8. Fahey JW, Haristoy X, Dolan PM, et al. Sulforaphane inhibits extracellular, intracellular, and antibiotic-resistant strains of *Helicobacter pylori* and prevents benzo[*a*]pyrene-induced stomach tumors. *Proc Natl Acad Sci USA* 2002;99:7610–7615. [PubMed: 12032331]
9. Conaway CC, Wang CX, Pittman B, et al. Phenethyl isothiocyanate and sulforaphane and their N-acetylcysteine conjugates inhibit malignant progression of lung adenomas induced by tobacco carcinogens in A/J mice. *Cancer Res* 2005;65:8548–8557. [PubMed: 16166336]
10. Gamet-Payrastre L, Li P, Lumeau S, et al. Sulforaphane, a naturally occurring isothiocyanate, induces cell cycle arrest and apoptosis in HT29 human colon cancer cells. *Cancer Res* 2000;60:1426–1433. [PubMed: 10728709]
11. Jackson SJT, Singletary KW. Sulforaphane: a naturally occurring mammary carcinoma mitotic inhibitor, which disrupts tubulin polymerization. *Carcinogenesis* 2004;25:219–227. [PubMed: 14578157]
12. Xu C, Shen G, Chen C, Gelinas C, Kong AN. Suppression of NF-kappaB and NF-kappaB-regulated gene expression by sulforaphane and PEITC through IkappaBalpha, IKK pathway in human prostate cancer PC-3 cells. *Oncogene* 2005;24:4486–4495. [PubMed: 15856023]
13. Singh AV, Xiao D, Lew KL, Dhir R, Singh SV. Sulforaphane induces caspase-mediated apoptosis in cultured PC-3 human prostate cancer cells and retards growth of PC-3 xenografts *in vivo*. *Carcinogenesis* 2004;25:83–90. [PubMed: 14514658]
14. Myzak MC, Tong P, Dashwood WM, Dashwood RH, Ho E. Sulforaphane retards the growth of human PC-3 xenografts and inhibits HDAC activity in human subjects. *Exp Biol Med* 2007;232:227–234.
15. Singh SV, Warin R, Xiao D, et al. Sulforaphane inhibits prostate carcinogenesis and pulmonary metastasis in TRAMP mice in association with increased cytotoxicity of natural killer cells. *Cancer Res* 2009;69:2117–2125. [PubMed: 19223537]
16. Singh SV, Herman-Antosiewicz A, Singh AV, et al. Sulforaphane-induced G₂/M phase cell cycle arrest involves checkpoint kinase 2 mediated phosphorylation of Cdc25C. *J Biol Chem* 2004;279:25813–25822. [PubMed: 15073169]
17. Choi S, Singh SV. Bax and Bak are required for apoptosis induction by sulforaphane, a cruciferous vegetable derived cancer chemopreventive agent. *Cancer Res* 2005;65:2035–2043. [PubMed: 15753404]
18. Myzak MC, Hardin K, Wang R, Dashwood RH, Ho E. Sulforaphane inhibits histone deacetylase activity in BPH-1, LNCaP and PC-3 prostate epithelial cells. *Carcinogenesis* 2006;27:811–819. [PubMed: 16280330]
19. Mi L, Wang X, Govind S, et al. The role of protein binding in induction of apoptosis by phenethyl isothiocyanate and sulforaphane in human non-small lung cancer cells. *Cancer Res* 2007;67:6409–6416. [PubMed: 17616701]
20. Singh SV, Srivastava SK, Choi S, et al. Sulforaphane-induced cell death in human prostate cancer cells is initiated by reactive oxygen species. *J Biol Chem* 2005;280:19911–19924. [PubMed: 15764812]
21. Xiao D, Powolny AA, Antosiewicz J, et al. Cellular responses to dietary cancer chemopreventive agent D,L-sulforaphane in human prostate cancer cells are initiated by mitochondrial reactive oxygen species. *Pharmaceut Res* 2009;26:1729–1738.
22. Kim SH, Singh SV. D,L-sulforaphane causes transcriptional repression of androgen receptor in human prostate cancer cells. *Mol Cancer Ther* 2009;8:1946–1954. [PubMed: 19584240]

23. Aggarwal BB, Kunnumakkara AB, Harikumar KB, et al. Signal transducer and activator of transcription-3, inflammation, and cancer: How intimate is the relationship? *Ann NY Acad Sci* 2009;1171:59–76. [PubMed: 19723038]
24. Barton BE, Karras JG, Murphy TF, Barton A, Huang HF. Signal transducer and activator of transcription 3 (STAT3) activation in prostate cancer: Direct STAT3 inhibition induces apoptosis in prostate cancer lines. *Mol Cancer Ther* 2004;3:11–20. [PubMed: 14749471]
25. Tam L, McGlynn LM, Traynor P, Mukherjee R, Bartlett JM, Edwards J. Expression levels of the JAK/STAT pathway in the transition from hormone-sensitive to hormone-refractory prostate cancer. *Br J Cancer* 2007;97:378–383. [PubMed: 17595657]
26. Herman-Antosiewicz A, Xiao H, Lew KL, Singh SV. Induction of p21 protein protects against sulforaphane-induced mitotic arrest in LNCaP human prostate cancer cell line. *Mol Cancer Ther* 2007;6:1673–1681. [PubMed: 17513615]
27. Xiao D, Srivastava SK, Lew KL, et al. Allyl isothiocyanate, a constituent of cruciferous vegetables, inhibits proliferation of human prostate cancer cells by causing G₂/M arrest and inducing apoptosis. *Carcinogenesis* 2003;24:891–897. [PubMed: 12771033]
28. Ahn KS, Sethi G, Sung B, Goel A, Ralhan R, Aggarwal BB. Guggulsterone, a farnesoid X receptor antagonist, inhibits constitutive and inducible STAT3 activation through induction of a protein tyrosine phosphatase SHP-1. *Cancer Res* 2008;68:4406–4415. [PubMed: 18519703]
29. Shin DS, Kim HN, Shin KD, et al. Cryptotanshinone inhibits constitutive signal transducer and activator of transcription 3 function through blocking the dimerization in DU145 prostate cancer cells. *Cancer Res* 2009;69:193–202. [PubMed: 19118003]
30. Heinrich PC, Behrmann I, Müller-Newen G, Schaper F, Graeve L. Interleukin-6-type cytokine signalling through the gp130/Jak/STAT pathway. *Biochem J* 1998;334:297–314. [PubMed: 9716487]
31. Darnell JE Jr. STATs and gene regulation. *Science* 1997;277:1630–1635. [PubMed: 9287210]
32. Mora LB, Buettner R, Seigne J, et al. Constitutive activation of Stat3 in human prostate tumors and cell lines: direct inhibition of Stat3 signaling induces apoptosis of prostate cancer cells. *Cancer Res* 2002;62:6659–6666. [PubMed: 12438264]
33. Dhir R, Ni Z, Lou W, DeMiguel F, Grandis JR, Gao AC. Stat3 activation in prostatic carcinomas. *Prostate* 2002;51:241–246. [PubMed: 11987152]
34. Huang HF, Murphy TF, Shu P, Barton AB, Barton BE. Stable expression of constitutively-activated STAT3 in benign prostatic epithelial cells changes their phenotype to that resembling malignant cells. *Mol Cancer* 2005;4:2–8. [PubMed: 15647107]
35. Horinaga M, Okita H, Nakashima J, Kanao K, Sakamoto M, Murai M. Clinical and pathologic significance of activation of signal transducer and activator of transcription 3 in prostate cancer. *Urology* 2005;66:671–675. [PubMed: 16140113]
36. Lee SO, Lou W, Hou M, de Miguel F, Gerber L, Gao AC. Interleukin-6 promotes androgen-independent growth in LNCaP human prostate cancer cells. *Clin Cancer Res* 2003;9:370–376. [PubMed: 12538490]
37. Feldman BJ, Feldman D. The development of androgen-independent prostate cancer. *Nat Rev Cancer* 2001;1:34–45. [PubMed: 11900250]
38. Yu CI, Meyer DJ, Campbell GS, et al. Enhanced DNA binding activity of a Stat3-related protein in cells transformed by the Src oncoprotein. *Science* 1995;269:81–83. [PubMed: 7541555]
39. Lou W, Ni Z, Dyer K, Twardy DJ, Gao AC. Interleukin-6 induces prostate cancer cell growth accompanied by activation of STAT3 signaling pathway. *Prostate* 2000;42:239–242. [PubMed: 10639195]
40. Gong A, He M, Vanaja DK, Yin P, Karnes RJ, Young CYF. Phenethyl isothiocyanate inhibits STAT3 activation in prostate cancer cells. *Mol Nutr Food Res* 2009;53:878–886. [PubMed: 19437484]
41. Herman-Antosiewicz A, Johnson DE, Singh SV. Sulforaphane causes autophagy to inhibit release of cytochrome *c* and apoptosis in human prostate cancer cells. *Cancer Res* 2006;66:5828–5835. [PubMed: 16740722]
42. Bommarreddy A, Hahm ER, Xiao D, et al. Atg5 regulates phenethyl isothiocyanate-induced autophagic and apoptotic cell death in human prostate cancer cells. *Cancer Res* 2009;69:3704–3712. [PubMed: 19336571]

**Fig. 1.**

A, immunoblotting for pSTAT3 and total STAT3 using lysates from CWR22Rv1 (lane 1), DU145 (lane 2), PC-3 (lane 3), and LNCaP (lane 4) cells without or after treatment with 10 ng/mL IL6 for 30 min in serum starved cells (12 h starvation). B, immunoblotting for pSTAT3, total STAT3, pJAK2, and total JAK2 using lysates from DU145 cells treated for 6, 12, or 24 h with DMSO (control) or SFN (20 or 40 μmol/L). Immunoblotting for pSTAT3, total STAT3, pJAK2, and total JAK2 using lysates from (C) DU145 cells and (D) LNCaP cells treated for 24 h with 40 μmol/L SFN in the absence or presence of 10 ng/mL IL6. Cells were stimulated with IL6 at the end of incubation period. The blots were stripped and re-probed with anti-actin antibody to normalize for differences in protein level. Numbers on top of the immunoreactive

bands represent change in protein level relative to corresponding DMSO-treated control. Each experiment was repeated at least twice and representative data from one such experiment are shown.

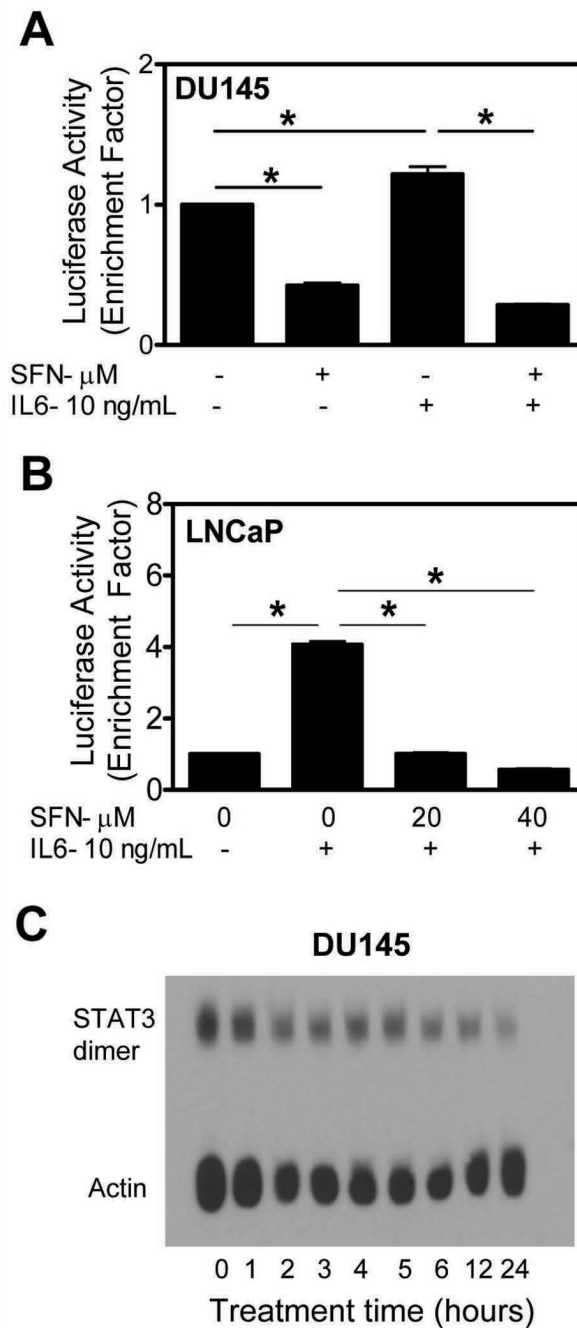


Fig. 2. Effect of 12 h treatment with the indicated concentrations of SFN on STAT3-associated luciferase activity in (A) DU145 cells and (B) LNCaP cells without or with 12 h stimulation with 10 ng/mL IL6. Columns, mean (n=3); bars, SE. *Significantly different ($P < 0.05$) between the indicated groups by one-way ANOVA followed by Bonferroni's multiple comparison test. C, analysis for STAT3 dimerization in DU145 cells treated with 40 μ mol/L SFN for the indicated time periods. Numbers on top of the immunoreactive bands represent fold change in STAT3 dimer level relative to control. Each experiment was repeated at least twice and representative data from one such experiment are shown.

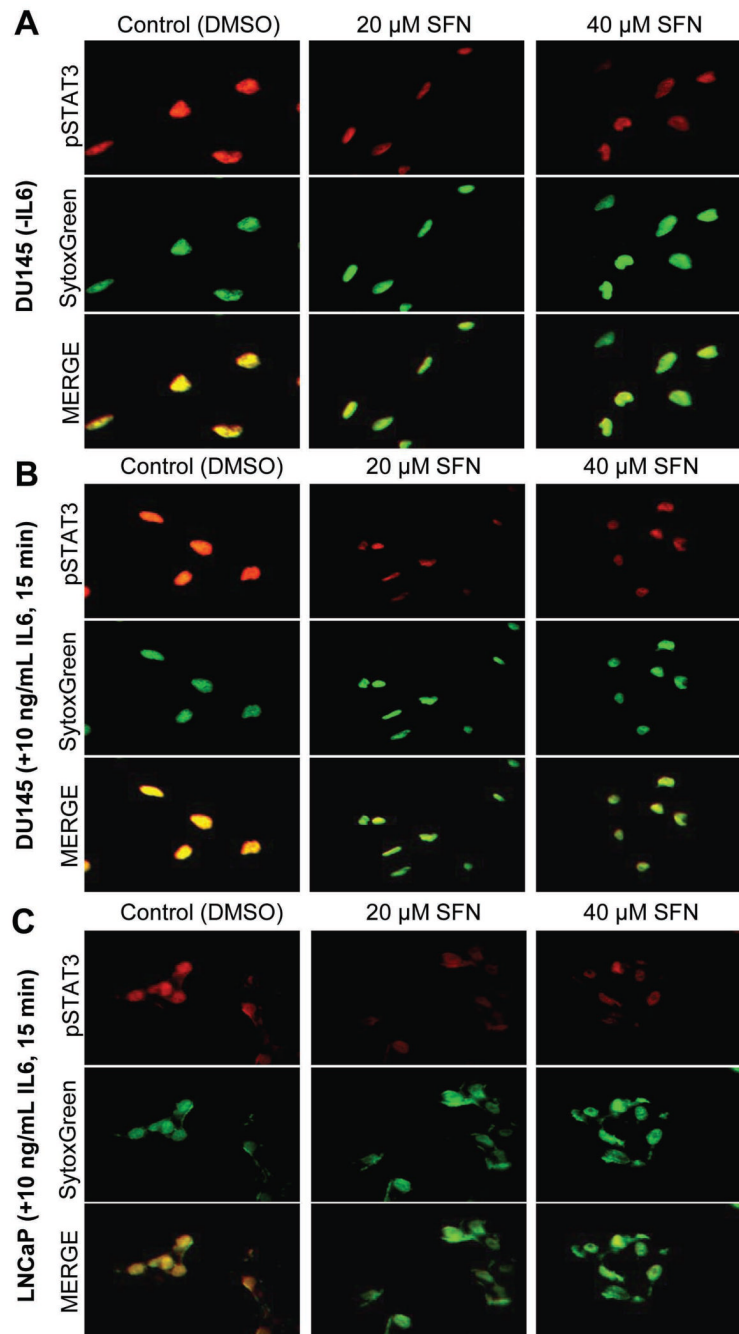


Fig. 3. DU145 (A,B) and LNCaP (C) cells were treated with SFN for 12 h. For stimulation, cells were exposed to IL6 for 15 min at the end of incubation period. The staining for pSTAT3 and nuclei is indicated by red and green fluorescence, respectively. Experiment was repeated twice and representative data from one such experiment are shown.

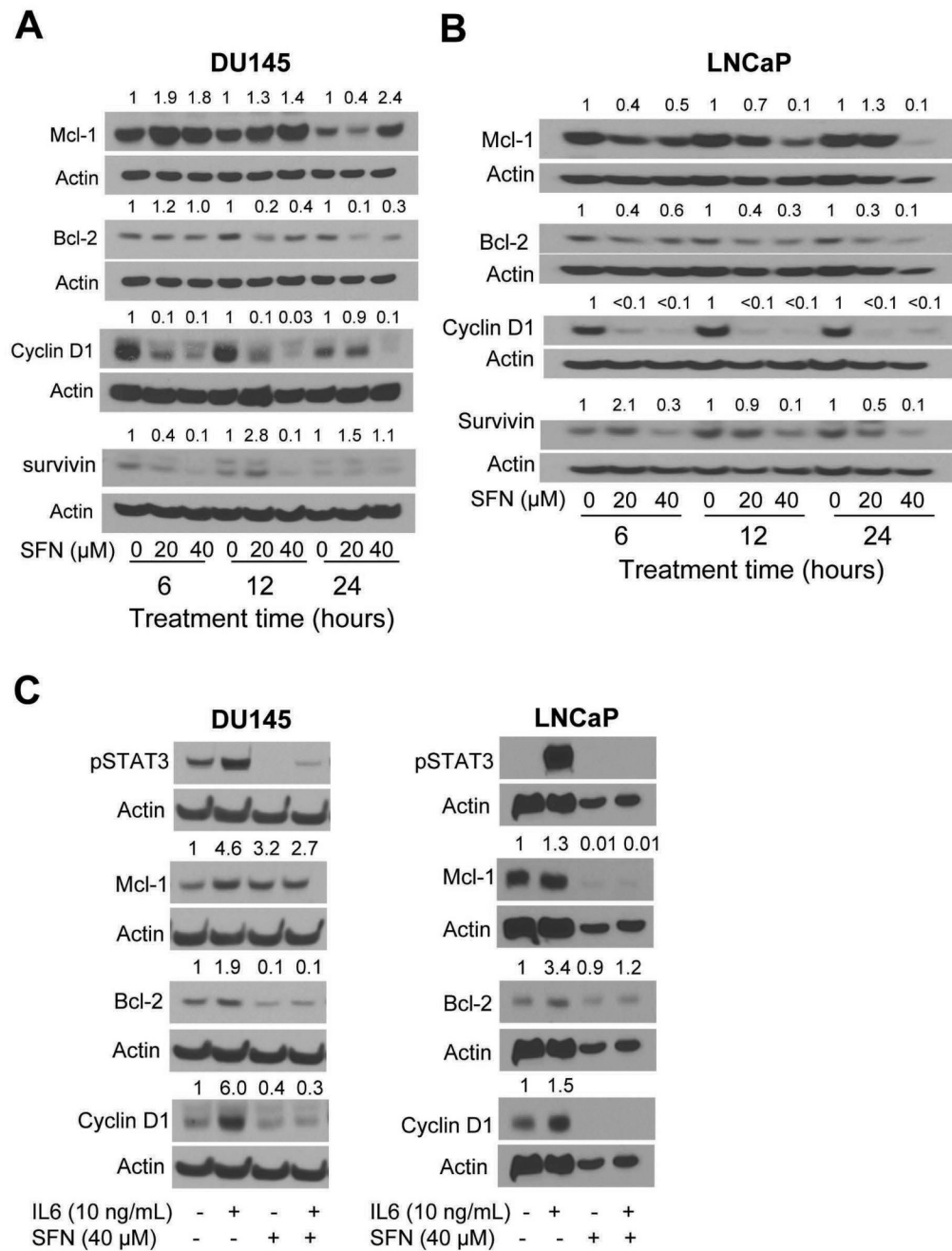


Fig. 4. Immunoblotting for Mcl-1, Bcl-2, Cyclin D1, and survivin using lysates from (A) DU145 cells and (B) LNCaP cells treated for 6, 12, or 24 with DMSO (control) or the indicated concentrations of SFN. C, immunoblotting for pSTAT3, Mcl-1, Bcl-2, and Cyclin D1 using lysates from DU145 and LNCaP cells treated for 24 h with 40 μmol/L SFN without or with 1 h stimulation (at the end of the 24 h incubation period) with 10 ng/mL IL6. The blots were stripped and re-probed with anti-actin antibody to normalize for differences in protein level. Numbers on top of the immunoreactive bands represent changes in protein levels relative to DMSO-treated control. Each immunoblotting experiment was repeated at least twice and representative data from one such experiment are shown.

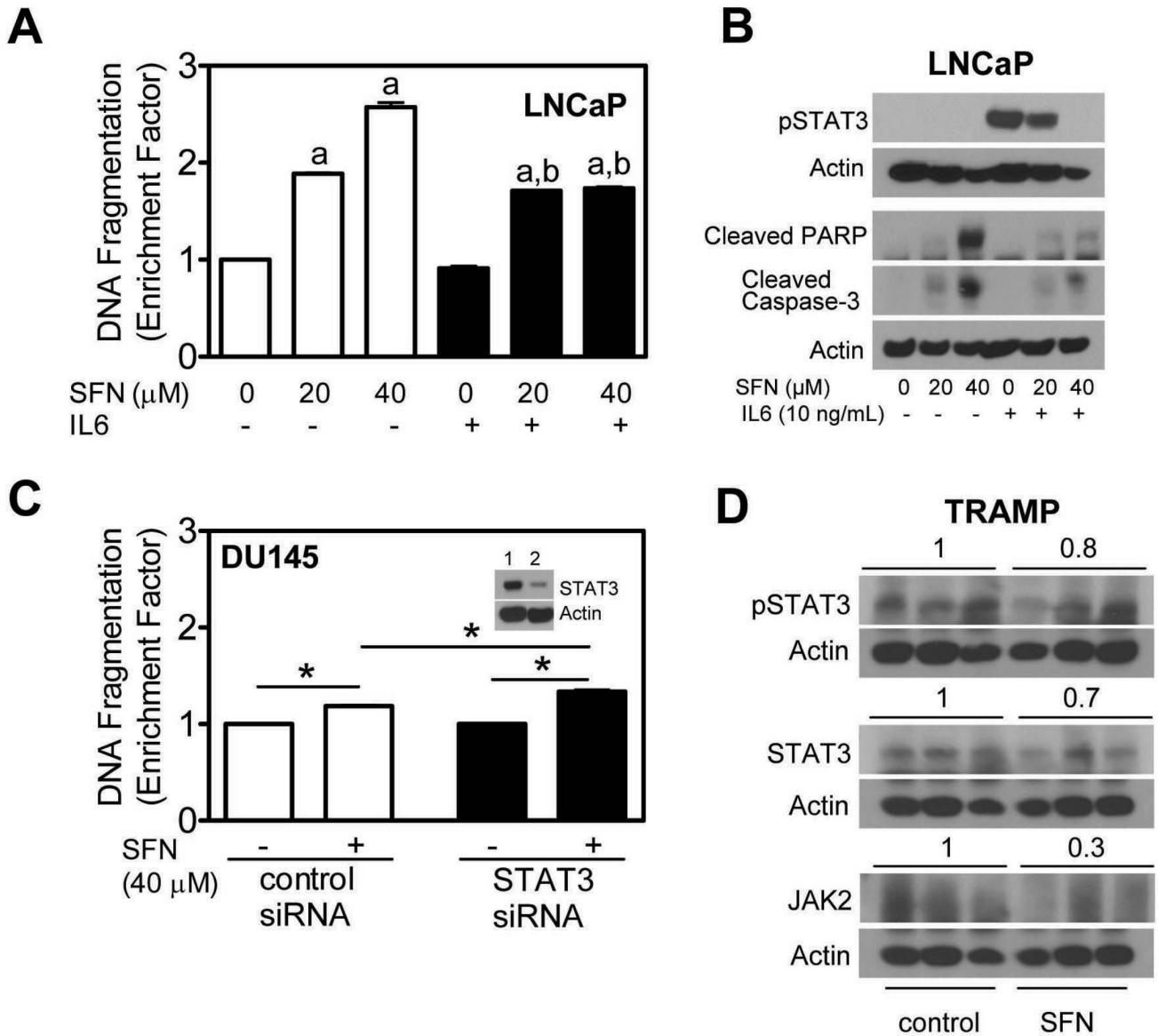
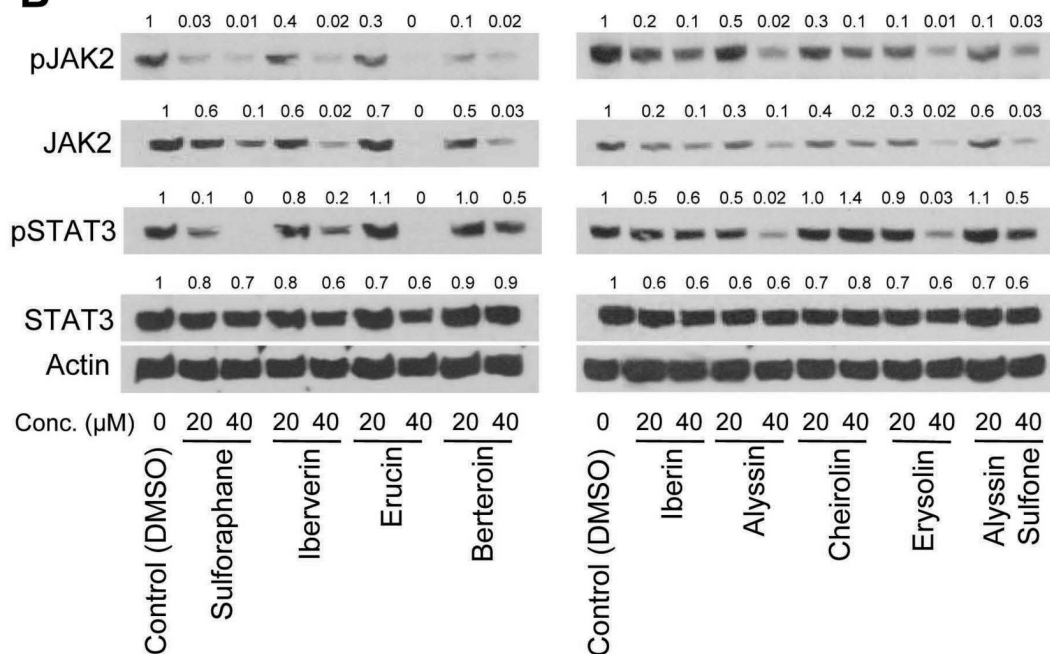


Fig. 5. A, analysis of cytoplasmic histone-associated DNA fragmentation in LNCaP cells following 24 h co-treatment with the indicated concentrations of SFN and 10 ng/mL IL6. *Columns*, mean (n=3); *bars*, SE. Significantly different ($P<0.05$) compared with ^arespective DMSO-treated control, and ^bDNA fragmentation in absence of IL6 stimulation by one-way ANOVA followed by Bonferroni's multiple comparison test. B, immunoblotting for pSTAT3, cleaved PARP, and cleaved caspase-3 using lysates from LNCaP cells following 24 h treatment with the indicated concentrations of SFN in the absence or presence of 10 ng/mL IL6 (24 h treatment). C, analysis of cytoplasmic histone-associated DNA fragmentation in DU145 cells transiently transfected with a control non-specific siRNA or STAT3-targeted siRNA and treated for 24 h with DMSO (control) or 40 μ mol/L SFN. *Inset*, immunoblotting for total STAT3 in cells transiently transfected with the nonspecific siRNA (lane 1) and the STAT3-targeted siRNA (lane 2). *Columns*, mean (n=3); *bars*, SE. *Significantly different ($P<0.05$) between the indicated groups by one-way ANOVA followed by Bonferroni's multiple comparison test. Experiments

were repeated at least twice and representative data from one such experiment are shown. *D*, immunoblotting for total and/or phospho-STAT3/JAK2 using supernatants from three representative prostate tumors harvested from control and SFN-treated TRAMP mice (15).

A

Chemical name	Common name	Chemical structure
3-(methylthio)-propyl isothiocyanate	Iberverin	$\text{CH}_3\text{-S-(CH}_2\text{)}_3\text{-N=C=S}$
4-(methylthio)-butyl isothiocyanate	Erucin	$\text{CH}_3\text{-S-(CH}_2\text{)}_4\text{-N=C=S}$
5-(methylthio)-pentyl isothiocyanate	Berteroin	$\text{CH}_3\text{-S-(CH}_2\text{)}_5\text{-N=C=S}$
3-(methylsulfinyl)-propyl isothiocyanate	Iberin	$\text{CH}_3\text{-SO-(CH}_2\text{)}_3\text{-N=C=S}$
4-(methylsulfinyl)-butyl isothiocyanate	Sulforaphane	$\text{CH}_3\text{-SO-(CH}_2\text{)}_4\text{-N=C=S}$
5-(methylsulfinyl)-pentyl isothiocyanate	Alyssin	$\text{CH}_3\text{-SO-(CH}_2\text{)}_5\text{-N=C=S}$
3-(methylsulfonyl)-propyl isothiocyanate	Cheirolin	$\text{CH}_3\text{-SO}_2\text{-(CH}_2\text{)}_3\text{-N=C=S}$
4-(methylsulfonyl)-butyl isothiocyanate	Erysolin	$\text{CH}_3\text{-SO}_2\text{-(CH}_2\text{)}_4\text{-N=C=S}$
5-(methylsulfonyl)-pentyl isothiocyanate	Alyssin sulfone	$\text{CH}_3\text{-SO}_2\text{-(CH}_2\text{)}_5\text{-N=C=S}$

B**Fig. 6.**

A, chemical structures of the SFN analogues used in the present study. *B*, immunoblotting for total and phosphorylated JAK2 and STAT3 using lysates from DU145 cells treated for 24 h with DMSO (control) or the indicated concentrations of SFN analogues. Numbers on top of the immunoreactive bands represent changes in protein levels relative to DMSO-treated control. Immunoblotting experiment was repeated 2–3 times with each analogue using independently prepared cell lysates. The results were consistent at the 40 $\mu\text{mol/L}$ dose but somewhat variable at the lower concentration.